



## FE analysis of extrusion defect and optimization of metal flow in porthole die for complex hollow aluminium profile

Jie YI<sup>1,2</sup>, Zhen-hu WANG<sup>1</sup>, Zhi-wen LIU<sup>1,3</sup>, Jian-ming ZHANG<sup>1,2</sup>, Xin HE<sup>1</sup>

1. State Key Laboratory of Advanced Design and Manufacture for Vehicle Body,  
Hunan University, Changsha 410082, China;

2. School of Mechanical Engineering, Hunan Industry Polytechnic, Changsha 410208, China;

3. School of Mechanical Engineering, University of South China, Hengyang 421001, China

Received 12 March 2018; accepted 13 June 2018

**Abstract:** To solve the defects of bottom concave appearing in the extrusion experiments of complex hollow aluminium profiles, a 3D finite element model for simulating steady-state porthole die extrusion process was established based on HyperXtrude software using Arbitrary Lagrangian–Eulerian (ALE) algorithm. The velocity distribution on the cross-section of the extrudate at the die exit and pressure distribution at different heights in the welding chamber were quantitatively analyzed. To obtain an uniformity of metal flow velocity at the die exit, the porthole die structure was optimized by adding baffle plates. After optimization, maximum displacement in the *Y* direction at the bottom of profile decreases from 1.1 to 0.15 mm, and the concave defects are remarkably improved. The research method provides an effective guidance for improving extrusion defects and optimizing the metal flow of complex hollow aluminium profiles during porthole die extrusion.

**Key words:** hollow aluminium profile; extrusion defect; metal flow velocity; baffle plate; ALE algorithm

### 1 Introduction

Aluminium alloys have lots of advantages and economic predominance in engineering because of their low density, high specific strength and specific stiffness, good collision energy absorption and recyclability [1,2], which are widely used in automobiles, rail transits, aerospace and construction. Extrusion is a highly efficient and low-energy-consumption process and is the main manufacturing procedure for hollow aluminium profiles. Thin-wall hollow aluminium profiles are usually extruded by the porthole dies [3]. Firstly, a billet is forced to flow through a splitter bridge and then split into multiple metal streams. Subsequently, the billet is allowed to flow into the welding chamber and welded each other under high temperature and pressure conditions. Finally, the billet is allowed to flow out of the die orifice between the die mandrel and the lower die to form hollow profiles of desired shape and size. The

higher the design complexity of the profile section is, the more inhomogenous the extrusion deformation is, and the more difficult to control the metal velocity at the die exit is.

The porthole die plays a key role in aluminum hollow profile production, which directly affects the product quality and service life of porthole die [4,5]. If the metal flow velocity on the cross-section of extrudate at the die exit is nonuniform, the performance and quality of extruded profiles will be seriously affected. In the traditional trial-and-error design, extrusion die design is mainly based on the practice experience and expertise of die designers [6]. Usually, after a porthole die is manufactured, it will undergo several modifications and tests until an acceptable profile is obtained, which causes additional cost and waste of time. With the rapid development of numerical technology, many researchers have performed some simulation work on aluminum alloy extrusion to provide accurate and theoretical guidance for die design [7]. CHEN et al [8] revealed the

material flow during multi-hole extrusion process for producing a hollow and thin-walled profile by means of numerical simulation based on the Arbitrary Lagrangian–Eulerian (ALE) algorithm. SUN et al [9] carried out the numerical simulation of extrusion process for a complex hollow magnesium doorframe using HyperXtrude software. BASTANI et al [10] performed a transient simulation of the aluminum extrusion process based on ALE algorithm in order to study how process parameters that influence flow balance and exit temperature. CHEN et al [11] carried out FE analysis on the extrusion process of a large hollow profile and modified the porthole die by reducing the area of porthole, adding baffle plate, and adjusting the length of bearing to obtain uniform velocity and temperature distributions of the extrudate. MAHMOODKHANI et al [12] investigated the influence of die feeder geometry on the formation of transverse weld using FE simulation.

In the present study, in order to solve the bottom concave defect of a complex hollow aluminum profile in the extrusion experiments, a 3D FE model for simulating the steady-state porthole die extrusion process was established based on HyperXtrude software using ALE algorithm. The velocity distribution on the cross-section of extrudate at die exit and pressure distribution in the welding chamber were quantitatively analyzed. The porthole die structure was optimized by adding baffle plates to obtain uniform metal flow velocity at the die exit. The research method and results are helpful to improve the extrusion defects of complex hollow aluminum profiles and optimize the porthole die structure.

## 2 Defects in initial extrusion experiment

The research object of this study is a complex hollow profile of 6063 aluminium alloy produced by an extrusion factory. Figure 1 shows the geometrical dimensions of the profile. The wall thickness of profile was 1–3 mm, the length and width dimensions were 107.46 and 62.62 mm, respectively. In actual extrusion experiments of the profiles, the bottom edge *B* of profile presents an inward depression that generates a small gap with the ruler, which is circled in red in Fig. 2. This defect is undetected with eye observation, but a noticeable depression can be observed when touching bottom edge *B*. As the reference, palpable depression is unnoticeable at position *C*.

## 3 Establishment of 3D FE model for porthole die extrusion

### 3.1 Geometry and FE modelling

Unigraphics NX software was used to establish the geometric model of the initial die design, extract the region boundary of metal flow through the container, portholes and welding chamber. Then, the model with Step format was imported into the HyperXtrude software for preprocessing. The geometrical model was divided into five parts: billet, porthole, welding chamber, die bearing and free surface. The basic principle of mesh generation was from small to large to ensure continuity of different parts of the extruded workpiece. The division order was as follows: die bearing, free surface, welding

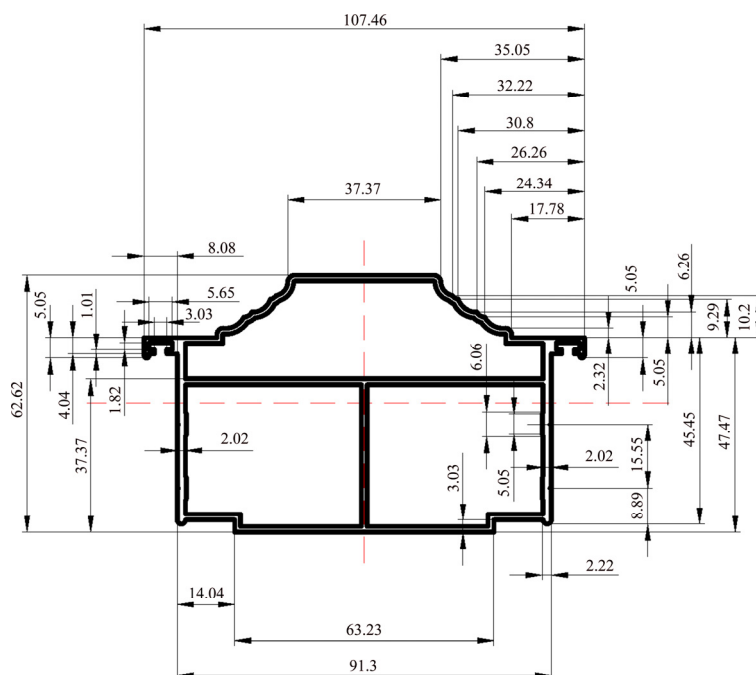


Fig. 1 Geometric dimensions of hollow profile (unit: mm)

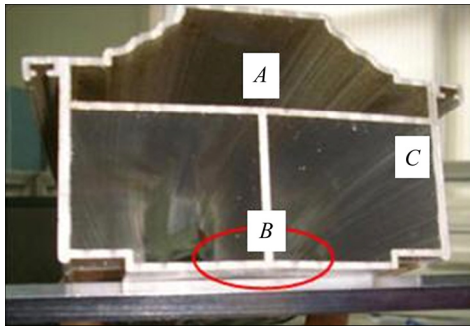


Fig. 2 Extrusion defects for initial porthole die

chamber, porthole and billet. To improve the accuracy and efficiency of FE simulations, the free surface length of extruded profile was set to be three times the length of die bearing, whereas the billet length is two times of the inner diameter of container. The pentahedron mesh was used in the components of profile and die bearing, while tetrahedron mesh was adopted in the billet, portholes and welding chamber. Die bearing was required to secure at least four free nodes in the thin area of the section. The mesh size was not larger than 1/5 of the size in the thinnest position, and mesh width should not be greater than 3 mm. Other parts were based on the mesh size of the die bearing. The mesh size of the welding chamber was 2.5 times of the die bearing, the mesh size of the portholes was three times of the welding chamber, and the mesh size of the billet was three times of the portholes. After mesh division, continuity between different mesh parts and their quality was checked. The ideal mesh quality must satisfy the following basic conditions: (1) minimum unit size >0.1 mm; (2) minimum unit angle >15°, maximum angle <165°; (3) length/width ratio of the unit: tetrahedron <8, triangular prism <12; (4) Jacobian >0.7. Figure 3 shows the FE model for steady die extrusion process of the hollow profiles.

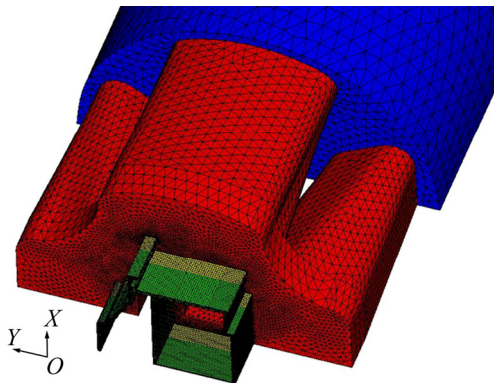


Fig. 3 FE model for steady die extrusion process of profiles

### 3.2 Material constitutive model

In the FE simulation of aluminium profile extrusion, the material was usually assumed to be an

incompressible viscous plastic non-Newtonian fluid. Figure 4 shows the flow stress curves of 6063 aluminium alloy at different temperatures and strain rates. In hot compression, the aluminium alloy possesses the same characteristics as that in high-temperature creep process, that is, thermal activation constantly occurs. The Sellars–Tegart model [13] was adopted in the simulation numerically to describe the behaviour of aluminium alloy. The material constitutive equations can be expressed as follows:

$$\sigma = \frac{1}{\beta} \sinh\left(\frac{Z}{A}\right)^{\frac{1}{n}} \quad (1)$$

$$Z = \dot{\epsilon} \exp[Q/(RT)] \quad (2)$$

where  $\sigma$  refers to material flow stress;  $Z$  corresponds to the Zener–Hollomon parameter;  $\dot{\epsilon}$  indicates the strain rate;  $A$ ,  $\beta$  and  $n$  are constants independent of temperature;  $R$  is the mole gas constant, 8.314 J/(mol·K);  $T$  is the thermodynamic temperature;  $Q$  denotes the deformation activation energy. The equations describe the balance between the work hardening and softening of temperature rise.

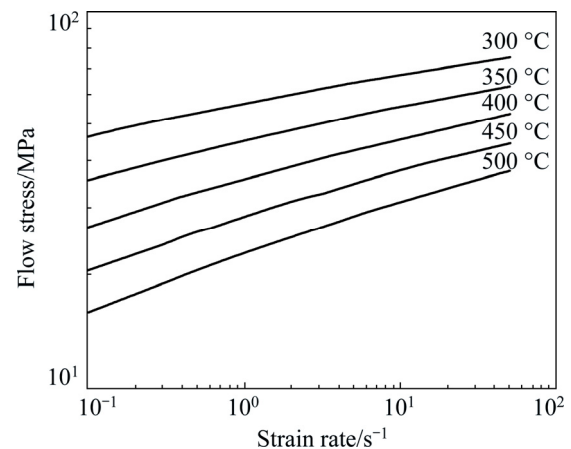


Fig. 4 Variation curves of flow stress of 6063 aluminium alloy with temperature and strain rate

In practical applications, the rheological stresses of the material can be determined under any deformation conditions when the values of  $A$ ,  $Q$ ,  $\alpha$  and  $n$  are given. In this study, the parameters of constitutive model for 6063 aluminium alloy were as follows:  $A = 5.91 \times 10^9 \text{ s}^{-1}$ ,  $Q = 1.415 \times 10^5 \text{ J/mol}$ ,  $n = 5.385$ ,  $\beta = 4 \times 10^{-8} \text{ m}^2/\text{N}$ .

### 3.3 Thermal boundary conditions and extrusion process parameters

Friction is an important factor that affects the metal flow of billet and temperature rise of the extrusion deformation. Existing research indicated that when the temperature was higher than 450 °C, the interface

frictions among the billet, the container and porthole die were considered to be adhesive friction type. In FE simulation, the friction coefficient ranged from 0.9 to 1, which can guarantee sufficient accuracy [14]. The friction between the billet and die bearing was defined as shear friction type. As shown in Eq. (3), friction coefficient is  $m$  ( $0 \leq m \leq 1$ ), and the friction coefficient was set to be 0.3 [15]. For the extrusion parameters, the initial time increment of FE simulation and nonlinear interaction tolerance were set to be 0.01 s and 0.001, respectively. The maximum nonlinear interaction was designated as 50.

$$\tau_f = m \left( \frac{\sigma}{\sqrt{3}} \right) \quad (3)$$

where  $\tau_f$  is shear friction coefficient, and  $\sigma$  is the equivalent flow stress.

During porthole die extrusion, the heat transfer of the billet, extrusion tools and the external environment significantly influences the metal flow and the extrusion temperature rise. The interface heat transfer coefficient of the container, porthole die and billet was specified as  $3000 \text{ W}/(\text{m}^2 \cdot ^\circ\text{C})$ , whereas that between the extruded profile and external environment was set to be  $20 \text{ W}/(\text{m}^2 \cdot ^\circ\text{C})$  [16]. The initial billet temperature was  $480 \text{ }^\circ\text{C}$  and the temperature of porthole die and container was  $30 \text{ }^\circ\text{C}$  lower than the billet temperature; the extrusion ratio was 29.69 and the extrusion speed was  $1 \text{ mm/s}$ . Table 1 shows the detailed extrusion process parameters and boundary conditions.

**Table 1** Process parameters and boundary conditions of porthole die extrusion

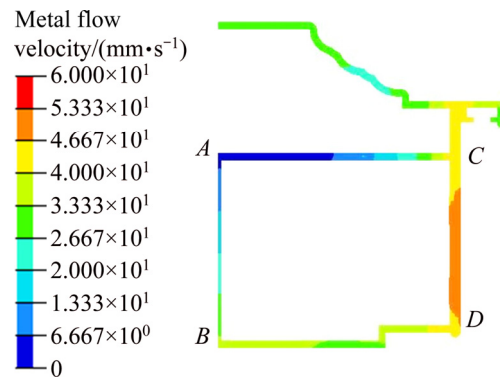
Parameter and condition	Value
Billet temperature/ $^\circ\text{C}$	480
Die and container temperature/ $^\circ\text{C}$	450
Extrusion speed/ $(\text{mm} \cdot \text{s}^{-1})$	1
Extrusion ratio	29.69
Friction coefficient between billet and container, porthole die	Full-sticking friction
Friction coefficient between billet and die bearing	0.3
Heat transfer coefficient with extrusion tools/ $(\text{W} \cdot \text{m}^{-2} \cdot ^\circ\text{C}^{-1})$	3000
Heat transfer coefficient with environment/ $(\text{W} \cdot \text{m}^{-2} \cdot ^\circ\text{C}^{-1})$	20

## 4 FE analysis of extrusion defects

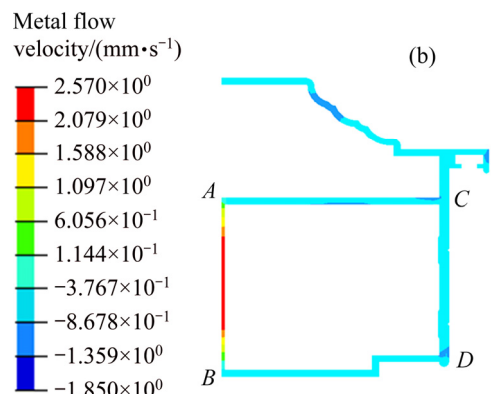
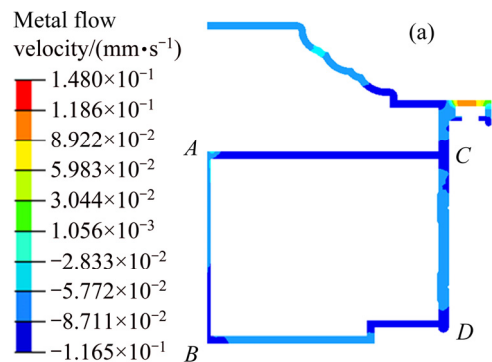
### 4.1 Metal flow velocity distribution at die exit

Figure 5 illustrates the metal flow velocity distribution on the cross-section of the extrudate along the extrusion direction. After extruding the metal through

the die bearing, a remarkable velocity difference is observed on the cross-section of profile. The deepest colour is observed at the centre part of extruded profile and the metal flow velocity is minimum. Other parts of the section exhibit higher flow velocity. The minimum velocity at point *A* is only  $5 \text{ mm/s}$ , whereas the velocities at points *B* and *C* are far higher than that of point *A*. The maximum velocity at point *C* is approximately  $40 \text{ mm/s}$ . The average velocity of point *B* at the bottom of profile is close to  $33 \text{ mm/s}$ . The velocity difference between point *A* and points *B*, *C* seriously hinders the metal flow towards the centre part of section. Further simulation results indicate that the metal flow velocity along the *X* direction (i.e. the *CA* direction) is close to zero (see Fig. 6(a)), and the average flow velocity of metal along



**Fig. 5** Distribution of metal flow velocity in *Z* direction on cross-section of extrudate along extrusion direction



**Fig. 6** Distribution of metal flow velocity on cross-section of extrudate: (a) *X* direction; (b) *Y* direction

the  $Y$  direction (i.e.  $BA$  direction) is 2.2 mm/s (see Fig. 6(b)). Therefore, the material at the bottom of profile flows along the  $Y$  direction. As a result, a concave defect on the bottom edge of profile appears in extrusion experiment.

#### 4.2 Pressure distribution in different directions

Figure 7 shows the pressure distributions of the billet along the extrusion direction in steady-state extrusion. It can be seen from Fig. 7(a) that, during the whole extrusion process, the pressure in the welding chamber is the highest, and gradually reduces from the billet to the die exit. Pressure distributions on different height sections were extracted from the top to the bottom of the welding chamber (see Figs. 7(b), (c), (d) and (e)). A uniform pressure distribution on the cross-section of workpiece is observed at the highest position of the welding chamber (see Fig. 7(b)). With the decrease of the

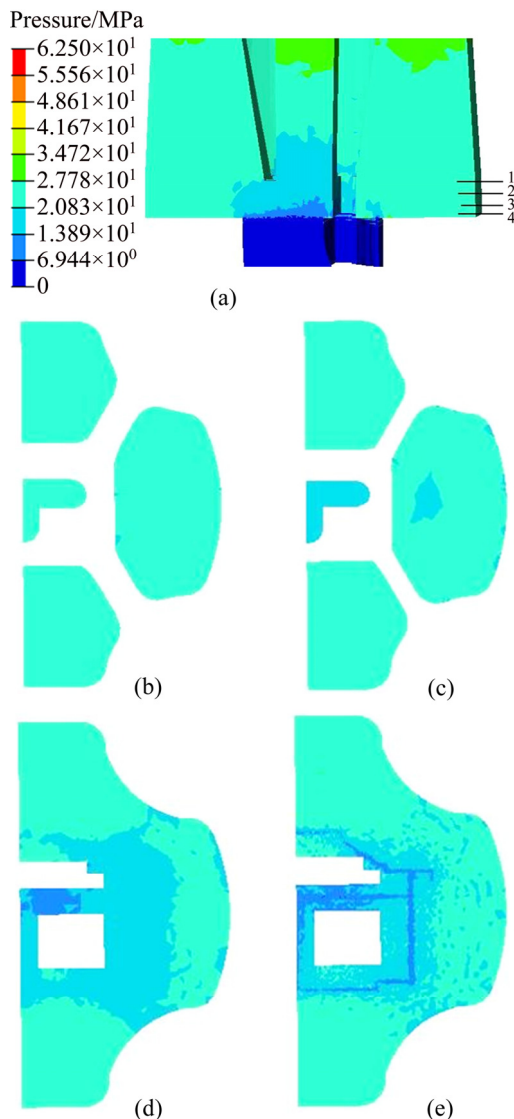


**Fig. 7** Pressure distributions of billets along extrusion direction during steady extrusion: (a) Steady state; (b) Cross-section 1; (c) Cross-section 2; (d) Cross-section 3; (e) Cross-section 4

section height, the pressure distribution of the welded metal gradually becomes non-uniform. The metal pressure in the centre part of workpiece first decreases, and the metal flow rate is the lowest. Secondly, the metal pressure corresponding to the  $AC$  edge decreases. Therefore, the slower part of the material on the edge of  $AC$  is greater than that of  $AB$ . Finally, the metal flows out the die orifice, whereas the pressure value reduces to zero. The preceding analysis indicates that the pressure distribution in the welding chamber influences the allocation of material and flow behavior. Flow velocity of the material with a small pressure is less than that with a large pressure, resulting in differences in velocity between the two parts.

## 5 Optimization of porthole die structure and test verification

### 5.1 Optimization of die structure

According to the previous analysis, the defect of the extruded profile is mainly attributed to the non-uniform metal flow on the cross-section of profile. According to the velocity distribution of the section, it is necessary to optimize the initial die structure. Adding baffle plates is an effective method for regulating flow velocity in the porthole die. This method is simple and feasible for use in baffle plates without reopening the die, which is the most common and first adopted repair measure. It is not necessary to redesign and machine the porthole die, and the repairing of the lower die is very simple and feasible. Therefore, to balance the metal flow velocity, baffle plates are added on the side with high flow velocity to increase the resistance of metal flow through the die orifice. Figure 8 shows the position distribution and dimensions of the baffle plates. The width and height of baffle plate are 6 and 5 mm, respectively. And the distance from the entrance of die orifice is 0.5 mm.

### 5.2 Metal flow velocity distribution at die exit

Figure 9 shows the metal flow velocity distribution on the cross-section of extrudate for the optimal porthole die. The metal flow velocity of point  $A$  remains the lowest and the average velocity increases to 19 mm/s. The minimum velocity is 7 mm/s, which is increased by 2 mm/s compared with that of the initial die. The flow velocity of points  $B$  and  $C$  from point  $A$  gradually increases. The average velocities of points  $B$  and  $C$  are 29 and 43 mm/s, respectively, which are decreased by 4 and 3 mm/s compared with the initial scheme. As a result, the metal flow velocity towards points  $B$  and  $C$  is slowed down by adding the baffle plates. However, the metal flow velocity at point  $A$  remains the same as that of the initial die scheme. Thus, the difference in the velocity between  $CA$  and  $BA$  reduces. Besides, the metal

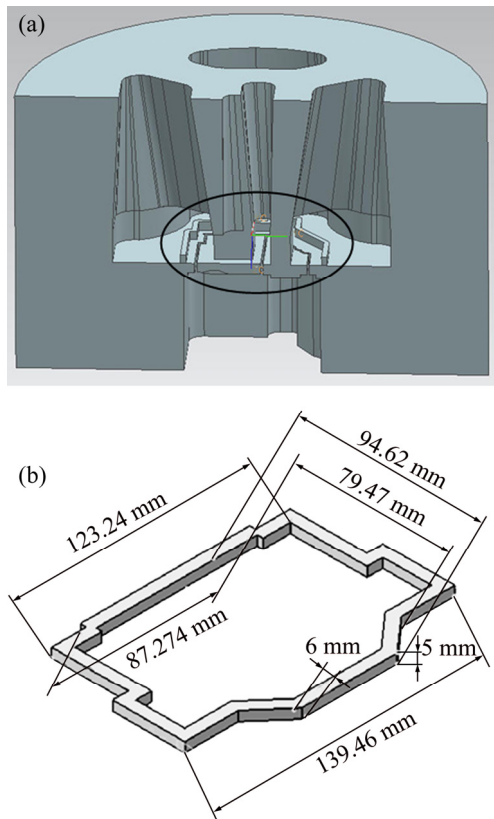


**Fig. 8** Modified porthole die: (a) Position of baffle plates; (b) Detail dimensions of baffle plates

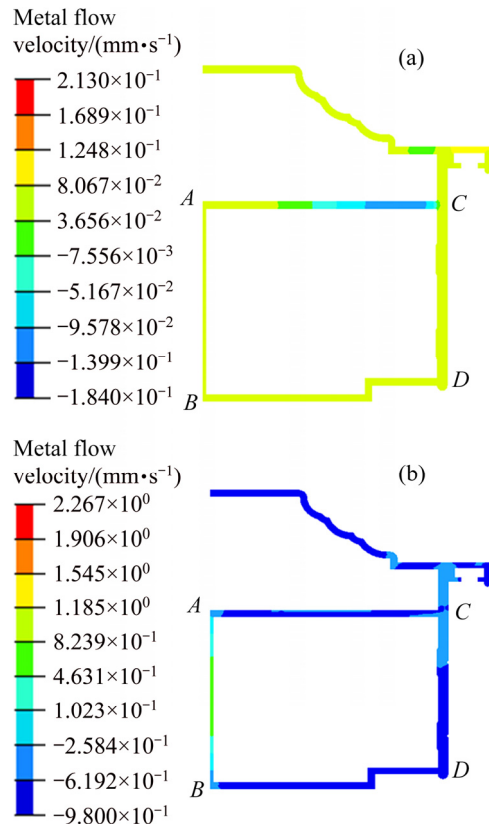


**Fig. 10** Distribution of metal flow velocity on cross-section of extrudate after optimization: (a) *X* direction; (b) *Y* direction

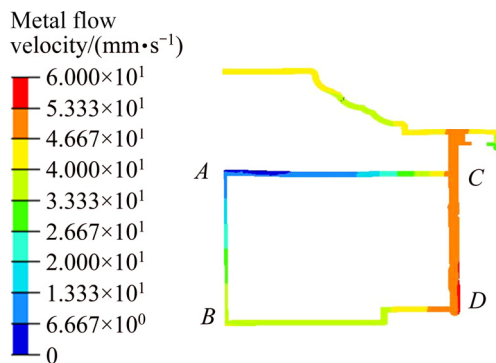


**Fig. 9** Distribution of metal flow velocity in *Z* direction on cross-section of extrudate after optimization

velocity distribution along the *X* direction (i.e. the *CA* direction) and *Y* direction (i.e. the *BA* direction) were extracted and shown in Fig. 10. It can be seen from Fig. 10 that the average metal flow velocity is close to zero in the *X* direction, indicating that no metal flow in the *X* direction. The average flow velocity of the metal along the *Y* direction is only 1 mm/s, which is 1.2 mm/s less than that in the initial design die. Therefore, the metal flow trend in the *Y* direction decreases.

### 5.3 Verification of extrusion experiments

Figure 11 shows the result of extrusion experiments for optimal porthole die. It can be seen that a sound

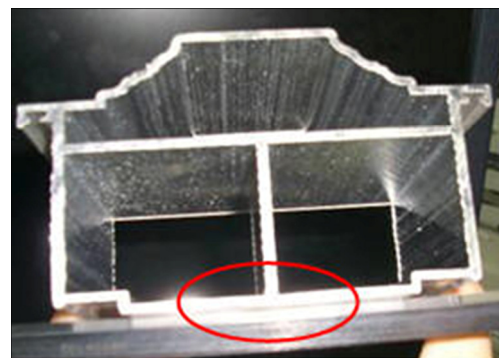


**Fig. 11** Extrusion experiment result after optimization of die structure

profile is produced and the concave defect is remarkably improved, which indicates that the baffle plates could effectively balance material flow during the porthole die extrusion process. After optimization, a relatively uniform flow velocity of metal at the die exit could be obtained. Figure 12 shows the comparison of measured displacements at the bottom of the profile before and after die modification (point *B* is the coordinate origin, *BA* is the *Y* axis, and the bottom edge *BD* is the *X* axis, see Fig. 9). Before optimization, the displacement at the bottom *B* is the largest, which is 1.1 mm. The farther the distance from point *B* is, the smaller the displacement of the profile is. This shows that the difference of the flow

velocity in the extrusion process is obvious. After adding the baffle plates, the displacement of the profile at point *B* is reduced to 0.15 mm and the farther the distance from point *B* is, the smaller the displacement reduction is, which indicates that the metal flow velocity in porthole die is more uniform after adding the baffle plates. This is mainly due to the increase of metal flow velocity at the center part of the section after adding the baffle plates, while that in external region of the section decreases. Thus, the velocity difference between inside and outside of the section decreases.

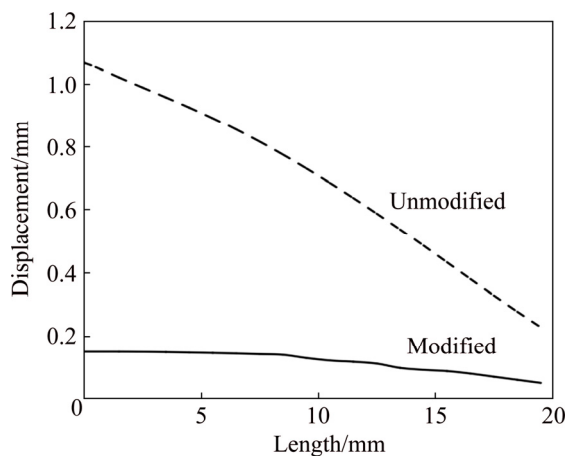


**Fig. 12** Comparison of measured displacements at bottom of profile before and after die modification

## 6 Conclusions

1) A 3D FE model for simulating steady-state porthole die extrusion of complex hollow aluminium profiles based on HyperXtrude software using ALE algorithm was established. The metal flow behavior and pressure distribution in different directions were investigated.

2) Visible metal flow velocity and pressure differences were observed in the centre part and the surrounding area of the profile section along the extrusion direction. The average metal velocity in the *Y* direction of *AB* edge was 2.2 mm/s, leading to a concave defect at the bottom of profile.

3) After addition of baffle plates in the lower die, the metal velocity in the centre part of the profile increases, whereas that in the external region of profile decreases. The metal velocity in the *Y* direction of *AB* edge reduces to 1 mm/s. As a result, the maximum displacement in *Y* direction at the bottom of profile reduces from 1.1 to 0.15 mm, and concave defect is remarkably improved.

## References

[1] LIU Zhi-wen, LI Luo-xing, YI Jie, LI Shi-kang, WANG Zhen-hu,

- WANG Guan. Influence of heat treatment conditions on bending characteristics of 6063 aluminum alloy sheets[J]. Transactions of Nonferrous Metals Society of China, 2017, 27(7): 1498–1506.
- [2] XIAO Gang, YANG Qin-wen, LI Luo-xing. Modeling constitutive relationship of 6013 aluminum alloy during hot plane strain compression based on Kriging method [J]. Transactions of Nonferrous Metals Society of China, 2016, 26(4): 1096–1104.
- [3] GUAN Yan-jin, ZHANG Cun-sheng, ZHAO Guo-qun, SUN Xue-mei, LI Peng. Design of a multihole porthole die for aluminum tube extrusion [J]. Materials and Manufacturing Processes, 2012, 27(2): 147–153.
- [4] CHEN L, ZHAO G Q, YU J Q. Effects of ram velocity on pyramid die extrusion of hollow aluminum profile [J]. International Journal of Advanced Manufacturing Technology, 2015, 79(9–12): 2117–2125.
- [5] ZHANG C S, ZHAO G Q, GUAN Y J, GAO A J, WANG L J, LI P. Virtual tryout and optimization of the extrusion die for an aluminum profile with complex cross-sections [J]. International Journal of Advanced Manufacturing Technology, 2015, 78(5–8): 927–937.
- [6] LIU P, XIE S S, CHENG L. Die structure optimization for a large, multi-cavity aluminum profile using numerical simulation and experiments [J]. Materials & Design, 2012, 36: 152–160.
- [7] LIU Z W, LI L X, YI J, LI S K, WANG G. Influence of extrusion speed on the seam weld quality in the porthole die extrusion of AZ31 magnesium tube [J]. The International Journal of Advanced Manufacturing Technology, 2017, 92(1–4): 1039–1052.
- [8] CHEN L, ZHAO G Q, YU J Q, ZHANG W D, WU T. Analysis and porthole die design for a multi-hole extrusion process of a hollow, thin-walled aluminum profile [J]. The International Journal of Advanced Manufacturing Technology, 2014, 74(1–4): 383–392.
- [9] SUN Y D, CHEN Q R, SUN W J. Numerical simulation of extrusion process and die structure optimization for a complex magnesium doorframe [J]. The International Journal of Advanced Manufacturing Technology, 2015, 80(1–4): 495–506.
- [10] BASTANI A F, AUKRUST T, SKAUVIK I. Study of flow balance and temperature evolution over multiple aluminum extrusion press cycles with HyperXtrude 9.0 [J]. Key Engineering Materials, 2010, 424: 257–264.
- [11] CHEN H, ZHAO G Q, ZHANG C S, GUAN Y J, LIU H, KOU F J. Numerical simulation of extrusion process and die structure optimization for a complex aluminum multicavity wallboard of high-speed train [J]. Materials and Manufacturing Processes, 2011, 26(12): 1530–1538.
- [12] MAHMOODKHANI Y, WELLS M A, PARSON N, POOLE W J. Numerical modelling of the material flow during extrusion of aluminium alloys and transverse weld formation [J]. Journal of Materials Processing Technology, 2014, 214(3): 688–700.
- [13] SELLARS C M, TEGART W J M G. Hot workability [J]. International Metallurgical Reviews, 1972, 17(1): 1–24.
- [14] den BAKKER A J, WERKHOVEN R J, SILLEKENS W H, KATGERMAN L. The origin of weld seam defects related to metal flow in the hot extrusion of aluminium alloys EN AW-6060 and EN AW-6082 [J]. Journal of Materials Processing Technology, 2014, 214(11): 2349–2358.
- [15] YU J Q, ZHAO G Q, CHEN L. Analysis of longitudinal weld seam defects and investigation of solid-state bonding criteria in porthole die extrusion process of aluminum alloy profiles [J]. Journal of Materials Processing Technology, 2016, 237: 31–47.
- [16] FANG G, ZHOU J, DUSZCZYK J. Extrusion of 7075 aluminium alloy through double-pocket dies to manufacture a complex profile [J]. Journal of Materials Processing Technology, 2009, 209(6): 3050–3059.

## 复杂空心铝型材的挤压缺陷仿真分析及材料在分流模中的流动行为优化

易杰<sup>1,2</sup>, 王震虎<sup>1</sup>, 刘志文<sup>1,3</sup>, 张见明<sup>1</sup>, 何芯<sup>1</sup>

1. 湖南大学 汽车车身先进设计制造国家重点实验室, 长沙 410082;

2. 湖南工业职业技术学院 机械工程学院, 长沙 410208;

3. 南华大学 机械工程学院, 衡阳 421001

**摘要:** 为了解决复杂空心铝型材在挤压试验中出现的截面内凹缺陷, 基于 Arbitrary Lagrangian–Eulerian (ALE)算法, 利用 HyperXtrude 软件平台建立型材在多孔分流挤压模具挤压过程中的三维稳态有限元模型。定量分析型材挤压出口不同方向的金属流速及焊合室内不同高度的压力分布。为实现出模口型材横截面材料流速的均匀性, 采用增加阻流块方法对模具结构进行优化。优化后进行挤压试验, 型材底面  $Y$  方向的最大位移由 1.1 mm 减小到 0.15 mm, 内凹缺陷得到显著改善。研究方法为复杂空心铝型材分流模挤压缺陷的改善和材料流动行为的优化提供理论指导。

**关键词:** 空心铝型材; 挤压缺陷; 材料流速; 阻流块; ALE 算法

(Edited by Wei-ping CHEN)